Advances in Materials Research, *Vol. 14, No. 4 (2025) 283-307*
https://doi.org/10.12989/amr.2025.14.4.283

Hygro-thermal vibration analysis of pre-/post-buckled FG-CNTRC nanobeams using nonlocal elasticity theory

Dang Van Hieu*[1], Nguyen Thi Hoa[2], Nguyen Thi Kim Thoa[2] and Bui Gia Phi[3]

[1]Faculty of Mechanical Engineering and Mechatronics, Phenikaa School of Engineering, Phenikaa University, Duongnoi, Hanoi, Vietnam
[2]Department of Applied Mechanics, Faculty of Vehicle and Energy Engineering, Thai Nguyen University of Technology, Tichluong, Thainguyen, Vietnam
[3]Faculty of Technical Fundamental, University of Transport Technology, Hanoi, Vietnam

(*Received May 15, 2025, Revised July 28, 2025, Accepted July 29, 2025*)

Abstract. This study presents an analytical investigation of the free vibration behavior of functionally graded carbon nanotube-reinforced composite nanobeams under hygro-thermal environments. The reinforcement of carbon nanotubes within the isotropic polymer matrix is considered in four distribution patterns: one uniform and three functionally graded distribution types. The material properties of both the carbon nanotubes and the matrix are assumed to be temperature-dependent, and the effective properties are estimated using the extended rule of mixtures. The governing equations are formulated based on the refined shear deformation beam theory in conjunction with nonlocal elasticity theory and are analytically solved for simply supported boundary conditions. The analytical results are first validated against available literature, and then extensive parametric studies are conducted to explore the effects of geometric dimensions, temperature and moisture levels, the nonlocal parameter, and various beam theories on the vibrational behavior of nanobeams.

Keywords: analytical solution; carbon nanotube; composite nanobeam; nonlocal elasticity; vibration

1. Introduction

Since their identification in 1991 by Iijima (1991), carbon nanotubes (CNTs) have been the focus of extensive research in numerous scientific and engineering disciplines due to their remarkable mechanical and physical characteristics. CNTs are cylindrical nanostructures composed of carbon atoms arranged in a hexagonal lattice, similar to graphene. They are classified into two main types: single-walled carbon nanotubes (SWCNTs) and multi-walled carbon nanotubes (MWCNTs). Due to their unique structure, CNTs exhibit a wide range of remarkable mechanical, thermal and electrical properties (Coleman *et al.* 2006, Thostenson *et al.* 2001). Regarding mechanical properties, CNTs exhibit tensile strength up to ~100 GPa, far surpassing that of steel. Young's modulus of CNTs can reach approximately 1 TPa. Thermal properties of CNTs are also outstanding: SWCNTs have thermal conductivity values up to 3000 - 6000 W/m·K, CNTs can withstand temperatures above 2800°C in vacuum conditions. CNTs exhibit outstanding electrical properties that make them highly

*Corresponding author, Ph.D., E-mail: hieu.dangvan@phenikaa-uni.edu.vn

http://www.techno-press.org/?journal=amr&subpage=5 ISSN: 2234-0912 (Print), 2234-179X (Online)

attractive for applications in nanoelectronics and advanced materials. CNTs possess an exceptionally high current carrying capacity - on the order of 10^9 A/cm² - greatly surpassing that of traditional metallic materials such as copper. Due to their extraordinarily high length-to-diameter ratios - often on the order of millions - CNTs exhibit unique mechanical and physical properties not seen in conventional materials. Outstanding mechanical and physical properties coupled with low density make CNTs well suited for use as reinforcing materials in advanced composite structures. Owing to their exceptional mechanical and physical properties, CNTs have found widespread applications across various fields such as electronics, energy storage devices, biomedical systems, environmental technologies, automotive and aerospace industries (Rao *et al.* 2024, Hughes *et al.* 2024).

Building upon the concept of functionally graded materials (FGMs), Shen (2009) proposed the idea of functionally graded carbon nanotube-reinforced composite (FG-CNTRC) materials, in which SWCNTs are aligned and functionally distributed within an isotropic polymer matrix according to predefined gradation rules. This approach aims to enhance the mechanical properties and achieve tailored structural responses. Inspired by Shen's pioneering contribution, significant attention has been devoted to investigating the mechanical behavior of FG-CNTRC structures. The nonlinear free vibration behavior of FG-CNTRC beams was studied by Ke *et al.* (2010). The Timoshenko beam theory and von-Kármán geometric nonlinearity assumptions are employed to derive the equations of motion for FG-CNTRC beams. Lin and Xiang (2014) employed the p-Ritz method to investigate the free vibration behavior of shear deformable FG-CNTRC beams. The large amplitude vibration, nonlinear bending and thermal postbuckling of FG-CNTRC beams resting on elastic foundation in thermal environments were investigated by Shen and Xiang (2013). The free vibration of laminated FG-CNTRC beams was investigated by Duy-Vo *et al.* (2019 using the first-order shear deformation beam theory and the finite element method. A two-step perturbation technique was proposed by Babaei *et al.* (2021) to examine the nonlinear vibration behavior of thermally pre-/post-buckled FG-CNTRC beams resting on a nonlinear elastic foundation. A general higher-order shear deformation beam model was employed to formulate the equations of motion of the beam. Based on a hyperbolic shear deformation beam theory, the bending and buckling behavior of FG-CNTRC beams were reported by Belarbi *et al.* (2021). The nonlinear flexural behaviors of FG-CNTRC laminated beams under a uniform pressure in thermal environments were investigated by Yang *et al.* (2020). Lin *et al.* (2021) investigated the free vibration, buckling, and dynamic stability of rotating pre-twisted FG-CNTRC beams with imperfections under thermal conditions. The first-order shear deformation beam theory was utilized by Xu *et al.* (2021) to study the free vibration behavior of rotating FG-CNTRC beams in thermal environments with general boundary conditions.

When CNTs are embedded into a polymer matrix, they give rise to a new class of advanced materials known as carbon nanotube-reinforced composites (CNTRCs). These composites exhibit a unique combination of low weight, high strength, and excellent thermal stability (Coleman *et al.* 2006, Thostenson *et al.* 2001). The mechanical performance of CNTRCs is significantly influenced by the dispersion, orientation, and volume fraction of CNTs, as well as their interaction with the surrounding matrix. In addition to uniformly distributed CNTs, researchers have proposed functionally graded distributions, where the CNT content varies continuously along the thickness (Shen 2009, Ke *et al.* 2010, Lin and Xiang 2014, Shen and Xiang 2013). This gradation enables better stress redistribution, improved interfacial bonding, and enhanced resistance to local failure. As a result, FG-CNTRCs are particularly attractive for applications where structural reliability and tunable material behavior are required, such as aerospace components, microscale actuators, and thermal barrier systems. However, due to their small scale and nonhomogeneous architecture, accurately modeling the mechanical response of CNTRCs presents significant challenges and

requires advanced theoretical frameworks.

Micro/nanostructures have diverse applications due to their unique properties. In microelectronics, they are crucial for microprocessors, sensors, and transistors, enhancing device efficiency (Zhang *et al.* 2025). In biomedicine, they enable drug delivery systems and biosensors (Wang *et al.* 2023, Limongi *et al.* 2017). They enhance energy storage in batteries and solar cells and are also employed in sensors and actuators for both environmental and industrial applications (Zhang *et al.* 2019, Owais *et al.* 2024). Furthermore, micro/nano structures reinforce composite materials for aerospace and automotive industries, and are essential in water purification, filtration, and environmental monitoring (Bhat *et al.* 2021, Khan *et al.* 2024). Additionally, they contribute to advancements in photonics and membrane technologies. In Micro-/Nano-Electro-Mechanical Systems (MEMS/NEMS), moving components play a crucial role in enabling sensing, actuation, signal processing, and mechanical motion at the micro/nanoscale. These components operate based on the interaction between mechanical forces and electrical signals, with several dominant actuation mechanisms being employed: electrostatic, thermal, piezoelectric, magnetic actuations (Zhang *et al.* 2014, Algamili *et al.* 2021, Pachkawade 2024). Movable components in MEMS/NEMS devices, such as micro/nanobeams, cantilevers, and membranes, enable mechanical responses through controlled deformation or displacement. Size-dependent behavior in micro and nanoscale structures arises due to physical phenomena that are not adequately captured by classical continuum mechanics. To accurately model the size-dependent behavior of micro and nanoscale structures, several higher-order elasticity theories have been developed beyond classical continuum mechanics, such as the nonlocal elasticity theory (Eringen 1983) the strain gradient theory (Mindlin 1964, 1965, Mindlin and Eshel 1968), the modified couple stress theory (Yang *et al.* 2002), and the nonlocal strain gradient theory (Lim *et al.* 2015). These advanced theories are essential for the precise analysis and design of small-scale structures, ensuring accurate predictions of deformation, vibration, and stability characteristics in emerging nanotechnology and micro-engineered systems (Roudbari *et al.* 2022, Chandel *et al.* 2020, Farajpour *et al.* 2018). Among the various higher-order elasticity theories developed to capture small-scale effects, the nonlocal elasticity theory proposed by Eringen (Eringen 1983) has proven particularly suitable for nanoscale structures. This theory introduces a length scale parameter into the constitutive relations, allowing the stress at a given point to depend not only on the local strain but also on the strains in its neighborhood. As a result, it can effectively describe the size-dependent softening behavior observed in nanostructures - an aspect that classical elasticity fails to capture. Compared with other advanced elasticity theories, such as the strain gradient theory (Mindlin 1964, 1965, Mindlin and Eshel 1968) or the modified couple stress theory (Yang *et al.* 2002), the nonlocal elasticity theory (Eringen 1983) offers a more straightforward mathematical framework and involves fewer additional material parameters. This simplicity facilitates analytical treatment and reduces computational cost, especially when coupled with refined beam theories. For these reasons, the nonlocal elasticity theory is adopted in this study to model the mechanical response of FG-CNTRC nanobeams subjected to hygro-thermal environments, where size effects and nonlocal interactions play a crucial role.

FG-CNTRC micro/nano structures provide significant advantages in applications that demand flexibility, high strength, and efficient performance at small scales. The study of the mechanical behavior of micro/nanobeams made from FG-CNTRC has attracted significant research interest. Based on the nonlocal strain gradient theory, the dynamic pull-in instability of FG-CNTRC nano-actuator considering damping impact was examined by Yang *et al.* (2016). Yang *et al.* (2017) investigated the size-dependent pull-in instability of FG-CNTRC piezoelectric tuning nano-actuator taking into account higher-order corrected electrostatic pressure as well as finite-temperature and

conductivity corrections of the Casimir force. The equation of motion of the nano-actuator was established based on the framework of Euler-Bernoulli beam theory and the nonlocal elasticity theory. Allahkarami and Nikkhah-Bahrami (2017) employed the modified couple stress theory and Timoshenko beam model to study the size-dependent vibration behavior of FG-CNTRC curved microbeams under axial magnetic field resting on elastic medium. The buckling and free vibration behaviors of FG-CNTRC-micro sandwich plate were investigated by Kolahdouzan *et al.* (2018) using the modified couple stress theory. Based on the first-order shear deformation plate theory and the nonlocal elasticity theory, the post-buckling analysis of FG-CNTRC microplate with a cut out subjected to a magnetic field and resting on an elastic medium was reported by Jamali *et al.* (2019). Arefi *et al.* (2019) studied the dynamic instability region of a sandwich piezoelectric nanobeam with FG-CNTRC face-sheets in the framework of the nonlocal strain gradient theory and various higher-order shear deformation beam theories. Thermo-electro-mechanical buckling characteristics of sandwich nanobeams with face-sheets made of FG-CNTRC based on the nonlocal strain gradient elasticity theory and various higher-order shear deformation beam theories were examined by Arani *et al.* (2019). The buckling and vibration behaviors of FG-CNTRC annular nanoplates were investigated by Kolahdouzan *et al.* (2020) using the differential quadrature method. The closed-form solutions for the static, buckling and free vibration analysis of FG-CNTRC nanobeams for some different boundary conditions were presented by Borjalilou *et al.* (2019) using the Timoshenko beam model combined with the nonlocal elasticity theory. The nonlinear free vibration behavior of FG-CNTRC microbeams with piezoelectric layers in thermal environments was investigated by Gia-Phi *et al.* (2022) using the nonlocal strain gradient theory and the Euler-Bernoulli beam model. Dehkordi and Beni (2023) investigated the free vibration behavior of FG-CNTRC Timoshenko microbeams, incorporating the effects of axial loading and bending–torsion coupling, within the framework of the modified couple stress theory. Abdelrahman *et al.* (2023) employed the nonlocal strain gradient theory to develop a size-dependent model for investigating the dynamic response of FG-CNTRC nanobeam resting on a two-parameter elastic foundation under a moving load. The combined effects of shear deformation and small-scale influences on the nonlinear vibration behavior of FG-CNTRC nanobeams were analyzed by Taati *et al.* (2022) using the first-order shear deformation beam model and the nonlocal elasticity theory. Using modified couple stress theory, Uzun and Yaylı (2024) examined the size-dependent free vibration characteristics of FG-CNTRC nanowires/nanobeams with movable ends. The Lord–Shulman type generalized thermo-elasticity, incorporating fractional-order nonlocal theory, was employed by Li *et al.* (2024) to investigate the thermoelastic bending wave propagation characteristics of a nanocomposite microbeam simultaneously reinforced by graphene platelets and CNTs.

Micro- and nano-scale structures are highly sensitive to environmental conditions, particularly hygro-thermal effects - the combined influence of temperature and moisture. These factors can induce significant deformation through thermal expansion and moisture swelling, especially in heterogeneous or multilayered systems where mismatches in material properties lead to residual stresses, warping, or delamination. Hygro-thermal effects significantly influence the deformation and reliability of micro/nano structures due to size-dependent material behavior and dominant surface interactions. However, comprehensive models that capture these coupled effects across scales remain limited, highlighting the need for further investigation. Recently, the hygro-thermal effects on the mechanical behavior of small-scale structures have attracted the attention of scientists. The combined effects of moisture and temperature on the free vibration characteristics of FG nanobeams resting on elastic foundation were investigated by Ebrahimi and Barati (2016). Penna *et al.* (2021) investigated the bending behavior of porous FG nanobeams under hygro-thermo-

mechanical loadings. The buckling behavior of the porous FG nanobeam under hygro-thermal environments incorporating the surface effect was investigated by Li *et al.* (2021). Pham *et al.* (2024) investigated the impact of hygro-thermal environment on dynamic behavior of variable thickness FG porous microplates. The dynamic stability of porous FG beams subjected to hygro-thermal environments was analyzed by Zhang *et al.* (2023) using the nonlocal strain gradient theory. Pham *et al.* (2023) conducted a hygro-thermal vibration analysis of bidirectional FG porous nanobeams resting on an elastic foundation, employing the nonlocal strain gradient theory in conjunction with the finite element method. Zhang *et al.* (2022) conducted a comprehensive study on the vibration frequencies and wave propagation characteristics of multi-directionally FG-CNTRC nanobeams subjected to hygro-thermal conditions. Recently, Anh *et al.* (2024) reported the nonlocal static analysis of magneto-electro-elastic sandwich micro/nanoplates with an FG-CNT core, considering the effects of a hygro-thermal environment. The hygro-thermo-magnetically induced vibration of FG-CNTRC small-scale plate was investigated by Forooghi and Alibeigloo (2022) employing the nonlocal strain gradient theory.

This study presents, for the first time, a hygro-thermal free vibration analysis of pre- and post-buckled FG-CNTRC nanobeams within the framework of nonlocal elasticity theory. The governing equations of motion are derived using a refined shear deformation theory, which inherently accounts for shear effects without the need for shear correction factors. The material properties of the FG-CNTRC nanobeams are assumed to be temperature-dependent and graded through the thickness, with values estimated using an extended rule of mixtures based on micromechanical modeling. Four CNT reinforcement patterns within the polymer matrix are considered, including one uniform and three FG distributions, to investigate their effects on the structural behavior. The analytical solution is obtained by solving the governing equations of the nanobeams under simply-supported boundary conditions. The results are first validated by comparing them with existing data in the literature. Subsequently, numerical examples are provided to evaluate the influence of various parameters, such as hygrothermal loadings, nonlocal parameter, CNT volume fraction, and the length-to-thickness ratio, on the free vibration response of the nanobeam.

2. Models and formulas

2.1 FG-CNTRC nanobeam

Consider a functionally graded carbon nanotube-reinforced composite (FG-CNTRC) nanobeam with length L and thickness h in a hygro-thermal environment, as illustrated in Fig. 1(a). The nanobeam consists of a composite made from an isotropic polymer matrix reinforced with CNTs, which are assumed to be distributed along the thickness direction according to predefined grading patterns. As depicted in Fig. 1(b), both a uniform distribution (UD) and several functionally graded (FG) distributions of CNTs are taken into account. Specifically, three types of non-uniform CNT distributions are considered: FGO-CNTRC, FGX-CNTRC, and FGV-CNTRC.

To accurately predict the effective material properties of FG-CNTRCs, various micromechanical models have been proposed. Among these, the Mori–Tanaka model (Seidel and Lagoudas 2006, Li *et al.* 2007) and the Voigt model also known as the classical rule of mixtures (Anumandla and Gibson 2006, Esawi and Farag 2007), are the most employed. The Mori–Tanaka scheme provides a more rigorous homogenization approach suitable for composites with micro-sized reinforcements, while the rule of mixtures offers a simple and practical means of estimating overall mechanical properties

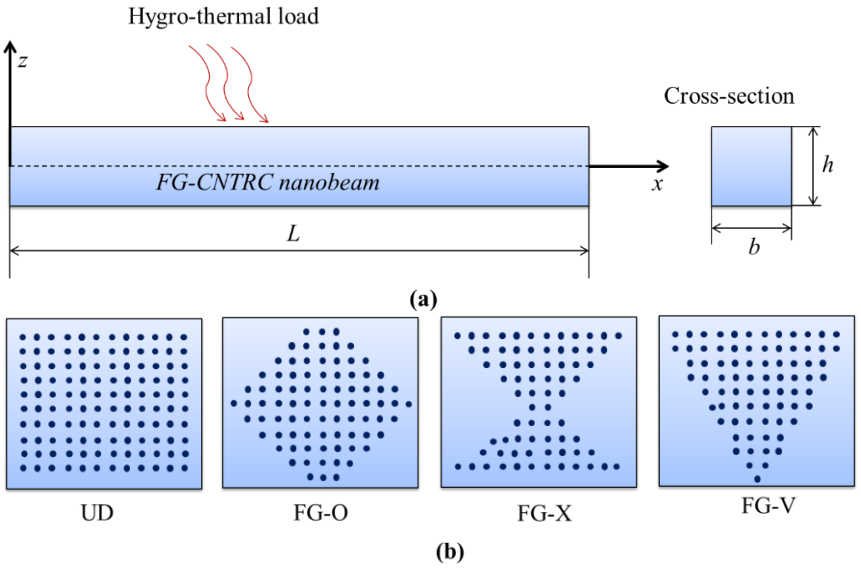

Fig. 1 Geometry of a nanobeam (a), and four different types of CNT distribution (b)

and structural responses. However, when applied at the nanoscale, both models must be modified to account for size-dependent effects, such as imperfect load transfer at the nanotube - matrix interface, surface energy influences, and nonlocal interactions. In this study, the extended rule of mixtures is adopted due to its balance between simplicity and adaptability to incorporate nanoscale phenomena. To this end, CNT efficiency parameters are introduced to modify the contribution of CNTs in the estimation of the composite's effective Young's moduli and shear modulus. It has been demonstrated in previous works that, when appropriately calibrated, both the extended Voigt and Mori–Tanaka models provide comparable accuracy in predicting the buckling and vibrational behavior of functionally graded ceramic–metal structures. Therefore, the extended rule of mixtures is employed herein as a reliable and computationally efficient approach to model the effective material behavior of FG-CNTRC nanobeams. Based on the extended rule of mixtures, the effective Young's modulus E_{11} and the shear modulus G_{12} can be expressed as (Shen 2009, Ke *et al.* 2010, Lin and Xiang 2014, Shen and Xiang 2013, Vo-Duy *et al.* 2019, Babaei *et al.* 2021, Belarbi *et al.* 2023, Yang *et al.* 2020):

$$E_{11} = \eta_1 V_{CNT} E_{11}^{CNT} + V_m E^m \tag{1}$$

$$\frac{\eta_2}{E_{22}} = \frac{V_{CNT}}{E_{22}^{CNT}} + \frac{V_m}{E^m} \tag{2}$$

$$\frac{\eta_3}{G_{12}} = \frac{V_{CNT}}{G_{12}^{CNT}} + \frac{V_m}{G^m} \tag{3}$$

where E_{11}^{CNT}, E_{22}^{CNT} and G_{12}^{CNT} are Young's moduli and shear modulus of the CNTs, respectively, and E^m and G^m represent respectively for Young's modulus and shear modulus of the isotropic polymer matrix. Due to the inherent mismatch in mechanical behavior at the nano - micro interface, the load transfer between the CNTs and the polymer matrix is generally imperfect. These

imperfections arise from several nanoscale phenomena, including surface effects, strain gradient influences and intermolecular stress coupling (Shen and Xiang 2013). To effectively capture these small-scale effects in the estimation of the composite's effective properties, efficiency parameters η_1, η_2 and η_3 are introduced into the extended rule of mixtures. The efficiency parameters η_1, η_2 and η_3 are subsequently calibrated by comparing the predicted moduli from the above expressions with those obtained through molecular dynamics simulations (Shen and Xiang 2013). V_{CNT} and V_m are the volume fractions of CNTs and isotropic polymer matrix, respectively, which are related by (Shen and Xiang 2013, Vo-Duy *et al.* 2019, Babaei *et al.* 2021, Belarbi *et al.* 2023, Yang *et al.* 2020):

$$V_{CNT} + V_m = 1 \tag{4}$$

The volume fraction of CNTs V_{CNT} corresponding to the four considered distribution patterns can be expressed as follows (Shen and Xiang 2013):

$$V_{CNT} = \begin{cases} V_{CNT}^{*} \text{(UD-CNTRC)} \\ 2\left(1 - \dfrac{2|z|}{h}\right) V_{CNT}^{*} \text{(FGO-CNTRC)} \\ 2\left(\dfrac{2|z|}{h}\right) V_{CNT}^{*} \text{(FGX-CNTRC)} \\ \left(1 + \dfrac{2z}{h}\right) V_{CNT}^{*} \text{(FGV-CNTRC)} \end{cases} \tag{5}$$

in which

$$V_{CNT}^{*} = \frac{w_{CNT}}{w_{CNT} + (\rho^{CNT}/\rho^{m}) - (\rho^{CNT}/\rho^{m}) w_{CNT}} \tag{6}$$

where w_{CNT} is the mass fraction of CNTs, and ρ^{CNT} and ρ^{m} are the densities of the CNTs and isotropic polymer matrix, respectively. It should be emphasized that, in this approach, the UD-CNTRC nanobeam, i.e., $V_{CNT} = V_{CNT}^{*}$, and the three types of FG-CNTRC nanobeams are designed to have the same total mass fraction of CNTs. It is important to note that, in contrast to the elastic properties, the load transfer between the CNTs and the polymer matrix does not influence the mass density of the CNTRC at any given location. Consequently, there is no need for a CNT efficiency parameter to modify the mass density of the CNTRC, which is defined as follows (Shen and Xiang 2013):

$$\rho = V_{CNT}\rho^{CNT} + V_m\rho^{m} \tag{7}$$

The Poisson's ratio depends weakly on temperature change and position and is expressed as:

$$\nu_{12} = V_{CNT}\nu_{12}^{CNT} + V_m\nu^{m} \tag{8}$$

The thermal expansion coefficient α_{11} is expressed as (Shen and Xiang 2013):

$$\alpha_{11} = \frac{E^{m}\alpha^{m}V_m + E_{11}^{CNT}\alpha_{11}^{CNT}V_{CNT}}{E^{m}V_m + E_{11}^{CNT}V_{CNT}} \tag{9}$$

where α_{11}^{CNT} and α^{m} are thermal expansion coefficients of the CNT and isotropic polymer matrix, respectively.

Furthermore, the moisture expansion coefficient of the nanocomposite, denoted as β, is assumed to be equal to that of the matrix material, β^{m}, based on the assumption that the polymer matrix fully absorbs the moisture content. Accordingly, the moisture expansion coefficient β can expressed as:

Table 1 Shape function

Beam theory	$f(z)$
Third-order beam theory (TBT)	$\frac{4z^3}{3h^2}$
Sinusoidal beam theory (SBT)	$z-\frac{h}{\pi}sin\left(\frac{\pi z}{h}\right)$
Exponential beam theory (EBT)	$z-ze^{-2\left(\frac{z}{h}\right)^2}$

$$\beta = \beta^m \tag{10}$$

2.2 The refined shear deformation beam theory

According to the refined shear deformation beam theory, the displacement field at any point of the nanobeam can be expressed as (Ebrahimi and Barati 2016):

$$\begin{aligned} u_1(x,z,t) &= u(x,t) - z\frac{dw_b(x,t)}{dx} + f(z)\frac{dw_s(x,t)}{dx} \\ u_2(x,z,t) &= 0 \\ u_3(x,z,t) &= w_b(x,t) + w_s(x,t) \end{aligned} \tag{11}$$

In this formulation, $u(x,t)$ denotes the longitudinal displacement, while $w_b(x,t)$ and $w_s(x,t)$ represent the bending and shear components of the transverse displacement, respectively, evaluated at a point on the nanobeam's midplane. The function $f(z)$ serves as the shape function, which characterizes the distribution of transverse shear strain and shear stress along the nanobeam's thickness. Various forms of $f(z)$ corresponding to different beam theories such as third-order, sinusoidal, and exponential - are summarized in Table 1. The non-zero strain components of the proposed nanobeam model are expressed as follows:

$$\varepsilon_{xx} = \frac{du}{dx} - z\frac{d^2w_b}{dx^2} - f\frac{d^2w_s}{dx^2}; \gamma_{xz} = (1-df/dz)\frac{dw_s}{dx} \tag{12}$$

To derive the equation of motion of the FG-CNTRC nanobeam, Hamilton's principle is employed:

$$\int_0^T (\delta U + \delta \Pi - \delta K)dt = 0 \tag{13}$$

where δU, $\delta \Pi$ and δK are the variation of the strain energy, potential energy and kinetic energy of the nanobeam, respectively. The variation of the strain energy of the FG-CNTRC nanobeam can be expressed as:

$$\delta U = \int_0^L (\sigma_{xx}\delta\varepsilon_{xx} + \sigma_{xz}\delta\gamma_{xz}dAdx = \int_0^L \left(N_{xx}\frac{d\delta u}{dx} - M_b\frac{d^2\delta w_b}{dx^2} - M_s\frac{d^2\delta w_s}{dx^2} + Q_{xz}\frac{d\delta w_s}{dx}\right)dx \tag{14}$$

in which, N_{xx}, M_b, M_s and Q_{xz} are the stress resultants which are defined as below:

$$(N_{xx}, M_b, M_s) = \int_A (1, z, f)\sigma_{xx}dA\,;\;\; Q_{xz} = \int_A (1-df/dz)\sigma_{xz}dA \tag{15}$$

The variation of the potential energy of the applied loads acting on the FG-CNTRC nanobeam is:

$$\delta\Pi = \int_0^L \left\{ (N^T + N^H) \left[\frac{d(w_b + w_s)}{dx} \frac{d\delta(w_b + w_s)}{dx} \right] \right\} dx \tag{16}$$

where N^T and N^H are applied forces due to temperature and moisture change which are determined as:

$$(N^T, N^H) = \int_{-h/2}^{h/2} Q_{11} (\alpha_{11}\Delta T, \beta\Delta H) dz \tag{17}$$

where $Q_{11} = E_{11}/(1 - \nu_{12}\nu_{21})$; $\Delta T = T - T_0$ and $\Delta H = H - H_0$ represent the increases in temperature and moisture, respectively, starting from the initial values of bottom surface temperature $T_0 = 300(K)$ and moisture content $H_0 = 0(\%wt.H_2O)$, respectively. It is important to note that, in this study, a uniform distribution of both temperature and moisture fields through the thickness is assumed:

$$T = T_0 + \Delta T; H = H_0 + \Delta H \tag{18}$$

The variation of the kinetic energy can be expressed as:

$$\delta K = \int_0^L \left\{ \begin{array}{l} I_0 \left[\frac{du}{dt}\frac{d\delta u}{dt} + \left(\frac{dw_b}{dt} + \frac{dw_s}{dt} \right) \left(\frac{d\delta w_b}{dt} + \frac{d\delta w_s}{dt} \right) \right] - I_1 \left(\frac{du}{dt}\frac{d^2\delta w_b}{dxdt} + \frac{d^2 w_b}{dxdt}\frac{d\delta u}{dt} \right) \\ + I_2 \left(\frac{d^2 w_b}{dxdt}\frac{d^2\delta w_b}{dxdt} \right) - J_1 \left(\frac{du}{dt}\frac{d^2 w_s}{dxdt} + \frac{d^2\delta w_s}{dxdt}\frac{d\delta u}{dt} \right) + K_2 \left(\frac{d^2 w_s}{dxdt}\frac{d^2\delta w_s}{dxdt} \right) \\ + J_2 \left(\frac{d^2 w_b}{dxdt}\frac{d^2\delta w_s}{dxdt} + \frac{d^2 w_s}{dxdt}\frac{d^2\delta w_b}{dxdt} \right) \end{array} \right\} dx \tag{19}$$

where $(I_0, I_1, J_1, I_2, J_2, K_2)$ are the mass inertias which are defined as follows:

$$(I_0, I_1, J_1, I_2, J_2, K_2) = \int_A (1, z, f, z^2, zf, f^2) \rho dA \tag{20}$$

Substituting Eqs. (14), (16) and (19) into Eq. (12), and performing integration by parts, leads to the following partial different equations of motion:

$$\frac{\partial N_{xx}}{\partial x} = I_0 \frac{\partial^2 u}{\partial t^2} - I_1 \frac{\partial^3 w_b}{\partial x \partial t^2} - J_1 \frac{\partial^3 w_s}{\partial x \partial t^2} \tag{21}$$

$$\begin{array}{l} \frac{\partial^2 M_b}{\partial x^2} = (N^T + N^H) \left(\frac{\partial^2 w_b}{\partial x^2} + \frac{\partial^2 w_s}{\partial x^2} \right) + I_0 \left(\frac{\partial^2 w_b}{\partial t^2} + \frac{\partial^2 w_s}{\partial t^2} \right) \\ + I_1 \frac{\partial^3 u}{\partial x \partial t^2} - I_2 \frac{\partial^4 w_b}{\partial x^2 \partial t^2} - J_2 \frac{\partial^4 w_s}{\partial x^2 \partial t^2} \end{array} \tag{22}$$

$$\begin{array}{l} \frac{\partial^2 M_s}{\partial x^2} + \frac{\partial Q_{xz}}{\partial t} = (N^T + N^H) \left(\frac{\partial^2 w_b}{\partial x^2} + \frac{\partial^2 w_s}{\partial x^2} \right) + I_0 \left(\frac{\partial^2 w_b}{\partial t^2} + \frac{\partial^2 w_s}{\partial t^2} \right) \\ + J_1 \frac{\partial^3 u}{\partial x \partial t^2} - J_2 \frac{\partial^4 w_b}{\partial x^2 \partial t^2} - K_2 \frac{\partial^4 w_s}{\partial x^2 \partial t^2} \end{array} \tag{23}$$

2.3 The nonlocal elasticity theory for FG-CNTRC nanobeam

The NET considers the influence of strains from surrounding points when calculating the stress at a specific location. This allows for more accurate predictions of mechanical responses in nanostructures, where traditional theories do not fully capture scale effects. According to the NET, the constitutive equations can be expressed as (Eringen 1983):

$$\begin{cases} \sigma_{xx} - \mu \dfrac{\partial^2 \sigma_{xx}}{dx^2} = Q_{11}\varepsilon_{xx} \\ \sigma_{xz} - \mu \dfrac{\partial^2 \sigma_{xz}}{dx^2} = Q_{55}\gamma_{xz} \end{cases} \tag{24}$$

in which, $Q_{55} = G_{12}$, $\mu = (e_0 a)^2$ is the nonlocal parameter, with $e_0$being a material constant and a is an internal characteristic length. σ_{xx} and σ_{xz} are the normal and tangential nonlocal stresses, respectively. Putting Eq. (12) into Eq. (24) and the subsequent results in Eq. (15), the stress resultants can be obtained as:

$$N_{xx} - \mu \frac{d^2 N_{xx}}{dx^2} = A\frac{du}{dx} - B\frac{d^2 w_b}{dx^2} - B_s \frac{d^2 w_s}{dx^2} \tag{25}$$

$$M_b - \mu \frac{d^2 M_b}{dx^2} = B\frac{du}{dx} - D\frac{d^2 w_b}{dx^2} - D_s \frac{d^2 w_s}{dx^2} \tag{26}$$

$$M_s - \mu \frac{d^2 M_s}{dx^2} = B_s\frac{du}{dx} - D_s\frac{d^2 w_b}{dx^2} - H_s \frac{d^2 w_s}{dx^2} \tag{27}$$

$$Q - \mu \frac{d^2 Q}{dx^2} = A_s \frac{dw_s}{dx} \tag{28}$$

where

$$(A, B, B_s, D, D_s, H_s) = \int_A (1, z, f, z^2, zf, f^2) Q_{11} dA \,, A_s = \int_A (1 - df/dz)^2 \, Q_{55} dA \tag{29}$$

Substituting Eqs. (25)-(28) into Eqs. (21)-(23), the motion equations of of the FG-CNTRC nanobeam in terms of displacements (u, w_b, w_s) can be obtained as follows

$$\begin{aligned} &A\frac{\partial^2 u}{\partial x^2} - B\frac{\partial^3 w_b}{\partial x^3} - B_s \frac{\partial^3 w_s}{\partial x^3} \\ &= I_0\left(\frac{\partial^2 u}{\partial t^2} - \mu\frac{\partial^4 u}{\partial x^2 \partial t^2}\right) - I_1\left(\frac{\partial^3 w_b}{\partial x \partial t^2} - \mu\frac{\partial^5 w_b}{\partial x^3 \partial t^2}\right) - J_1\left(\frac{\partial^3 w_s}{\partial x \partial t^2} - \mu\frac{\partial^5 w_s}{\partial x^3 \partial t^2}\right) \end{aligned} \tag{30}$$

$$\begin{aligned} &B\frac{\partial^3 u}{\partial x^3} - D\frac{\partial^4 w_b}{\partial x^4} - D_s\frac{\partial^4 w_s}{\partial x^4} - (N^T + N^H)\left[\left(\frac{\partial^2 w_b}{\partial x^2} + \frac{\partial^2 w_s}{\partial x^2}\right) - \mu\left(\frac{\partial^4 w_b}{\partial x^4} + \frac{\partial^4 w_s}{\partial x^4}\right)\right] = \\ &I_0\left[\left(\frac{\partial^2 w_b}{\partial t^2} + \frac{\partial^2 w_s}{\partial t^2}\right) - \mu\left(\frac{\partial^4 w_b}{\partial x^2 \partial t^2} + \frac{\partial^4 w_s}{\partial x^2 \partial t^2}\right)\right] + I_1\left(\frac{\partial^3 u}{\partial x \partial t^2} - \mu\frac{\partial^5 u}{\partial x^3 \partial t^2}\right) \\ &- I_2\left(\frac{\partial^4 w_b}{\partial x^2 \partial t^2} - \mu\frac{\partial^6 w_b}{\partial x^4 \partial t^2}\right) - J_2\left(\frac{\partial^4 w_s}{\partial x^2 \partial t^2} - \mu\frac{\partial^6 w_s}{\partial x^4 \partial t^2}\right) \end{aligned} \tag{31}$$

$$B\frac{\partial^3 u}{\partial x^3} - D\frac{\partial^4 w_b}{\partial x^4} - D_s\frac{\partial^4 w_s}{\partial x^4} - (N^T + N^H)\left[\left(\frac{\partial^2 w_b}{\partial x^2} + \frac{\partial^2 w_s}{\partial x^2}\right) - \mu\left(\frac{\partial^4 w_b}{\partial x^4} + \frac{\partial^4 w_s}{\partial x^4}\right)\right] =$$
$$I_0\left[\left(\frac{\partial^2 w_b}{\partial t^2} + \frac{\partial^2 w_s}{\partial t^2}\right) - \mu\left(\frac{\partial^4 w_b}{\partial x^2 \partial t^2} + \frac{\partial^4 w_s}{\partial x^2 \partial t^2}\right)\right] + I_1\left(\frac{\partial^3 u}{\partial x \partial t^2} - \mu\frac{\partial^5 u}{\partial x^3 \partial t^2}\right) \tag{32}$$
$$- I_2\left(\frac{\partial^4 w_b}{\partial x^2 \partial t^2} - \mu\frac{\partial^6 w_b}{\partial x^4 \partial t^2}\right) - J_2\left(\frac{\partial^4 w_s}{\partial x^2 \partial t^2} - \mu\frac{\partial^6 w_s}{\partial x^4 \partial t^2}\right)$$

3. Analytical solution

In this section, the Navier solution method is utilized to derive analytical expressions for the free vibration behavior of FG-CNTRC nanobeams subjected to simply supported boundary conditions. Accordingly, the displacement field is assumed in the following form:

$$u(x,t) = \sum_{n=1}^{\infty} U_n \cos(\alpha x) e^{i\omega_n t} \tag{33}$$

$$w_b(x,t) = \sum_{n=1}^{\infty} W_{bn} \sin(\alpha x) e^{i\omega_n t} \tag{34}$$

$$w_s(x,t) = \sum_{n=1}^{\infty} W_{sn} \sin(\alpha x) e^{i\omega_n t} \tag{35}$$

In these solutions, (U_n, W_{bn}, W_{sn}) are the unknown coefficients, $\alpha = n\pi/L$ is the half-wave number. Substituting the solutions given in Eqs. (33)-(35) into the governing equations of motion (30)-(32), it leads to:

$$\left\{\begin{bmatrix} k_{11} & k_{12} & k_{13} \\ k_{21} & k_{22} & k_{23} \\ k_{31} & k_{23} & k_{33} \end{bmatrix} - \omega_n^2 \begin{bmatrix} m_{11} & m_{12} & m_{13} \\ m_{21} & m_{22} & m_{23} \\ m_{31} & m_{23} & m_{33} \end{bmatrix}\right\}\begin{Bmatrix} U_n \\ W_{bn} \\ W_{sn} \end{Bmatrix} = \begin{pmatrix} 0 \\ 0 \\ 0 \end{pmatrix} \tag{36}$$

where:

$$\begin{aligned} &k_{11} = -A\alpha^2, \quad k_{12} = k_{21} = B\alpha^3, \quad k_{13} = k_{31} = B_s\alpha^3, \\ &k_{22} = -D\alpha^4 + (N^T + N^H)(\alpha^2 + \mu\alpha^4), \\ &k_{23} = k_{32} = -D_s\alpha^4 + (N^T + N^H)(\alpha^2 + \mu\alpha^4), \\ &k_{33} = -A_s\alpha^2 - H_s\alpha^4 + (N^T + N^H)(\alpha^2 + \mu\alpha^4), \end{aligned} \tag{37}$$

$$\begin{aligned} &m_{11} = -I_0(1 + \mu\alpha^2), \quad m_{12} = m_{21} = I_1(\alpha + \mu\alpha^3), \\ &m_{13} = m_{31} = J_1(\alpha + \mu\alpha^3), \quad m_{22} = -I_0(1 + \mu\alpha^2) - I_2(\alpha^2 + \mu\alpha^4), \\ &m_{23} = m_{32} = -I_0(1 + \mu\alpha^2) - J_2(\alpha^2 + \mu\alpha^4), \quad m_{33} = -I_0(1 + \mu\alpha^2) - K_2(\alpha^2 + \mu\alpha^4). \end{aligned} \tag{38}$$

By solving the generalized eigenvalue problem stated in Eq. (36), the natural frequencies of FG-CNTRC nanobeams can be computed.

Table 2 The CNT efficiency parameters for SWCNTs/PMMA nanocomposite (Lin and Xiang 2011, Shen and Xiang 2013, Babaei *et al.* 2021)

V_{CNT}^{*}	η_1	η_2	η_3
0.12	0.137	1.022	0.715
0.17	0.142	1.626	1.138
0.28	0.141	1.585	1.109

4. Numerical results and discussions

This section presents a comprehensive analysis of the free vibration behavior of FG-CNTRC nanobeams subjected to hygro-thermal environments. The proposed model accounts for the combined effects of temperature variation and moisture concentration on the material properties and structural response. Numerical simulations are carried out to investigate the influence of some key parameters, including the nonlocal parameter, the CNT distribution pattern, volume fraction of CNTs, length-to-thickness ratio, temperature rise and moisture concentration on the natural frequencies of the nanobeam. For this purpose, the nanobeams are composed of an isotropic polymer matrix, Poly Methyl Methacrylate (PMMA), reinforced with armchair (10,10) SWCNTs. The temperature-dependent properties of the PMMA are (Babaei *et al.* 2021, Yang *et al.* 2020, Shen 2016):

$$\begin{aligned} &E^m = (3.52 - 0.0034T - 0.142H)\text{GPa}, \ \alpha^m = 45(1 + 0.0005\Delta T) \times 10^{-6}/\text{K}, \\ &\rho^m = 1150\text{kg/m}^3, \quad \nu^m = 0.34, \quad \beta^m = 0.00268\ (wt.\%H_2O)^{-1} \end{aligned} \tag{39}$$

The temperature-dependent properties of the CNTs are given by (Shen 2016):

$$\begin{aligned} &E_{11}^{CNT} = (6.18387 - 0.00286T + 4.22867 \times 10^{-6}T^2 - 2.2724 \times 10^{-9}T^3)\text{TPa}, \\ &E_{22}^{CNT} = (7.75348 - 0.00358T + 5.30057 \times 10^{-6}T^2 - 2.84868 \times 10^{-9}T^3)\text{TPa}, \\ &G_{12}^{CNT} = (1.80126 + 7.7845 \times 10^{-4}T - 1.1279 \times 10^{-6}T^2 + 4.93484 \times 10^{-10}T^3)\text{TPa}, \\ &\alpha_{11}^{CNT} = (-1.12148 + 0.02289T - 2.88155 \times 10^{-5}T^2 + 1.13253 \times 10^{-8}T^3) \times 10^{-6}/\text{K}, \\ &\nu_{12}^{CNT} = 0.175, \quad \rho^{CNT} = 1400\text{kg/m}^3, \quad \beta^{CNT} = 0\ (wt.\%\ \text{H}_2O)^{-1} \end{aligned} \tag{40}$$

The CNT efficiency parameters $\eta_i (i = 1,2,3)$ for three volume fractions of CNTs are listed in Table 2 (Lin and Xiang 2011, Shen and Xiang 2013, Babaei *et al.* 2021).

To visually demonstrate the temperature dependency of the effective Young's modulus (E_{11}) of FG-CNTRC nanobeams, Fig. 2 presents its variation along the normalized thickness direction (*z/h*) for four CNT distribution types: UD, FG-V, FG-O, and FG-X, under different temperature conditions. As expected, the UD distribution results in a constant modulus across the thickness. In the FG-V distribution, the CNT content increases linearly from the bottom to the top surface, leading to a corresponding linear increase in E_{11}. The symmetric FG-O configuration yields the highest CNT concentration at the mid-plane, producing a maximum modulus at the center that decreases toward the surfaces. In contrast, the FG-X distribution concentrates CNTs near the top and bottom surfaces, resulting in a minimum E_{11} at the center and higher values near the outer layers. In all configurations, the effective Young's modulus noticeably decreases with increasing temperature, confirming the strong thermal sensitivity of the material.

The dimensionless natural frequency is introduced as:

$$\Omega = \omega(L^2/h)\sqrt{\rho_0^m/E_0^m} \tag{41}$$

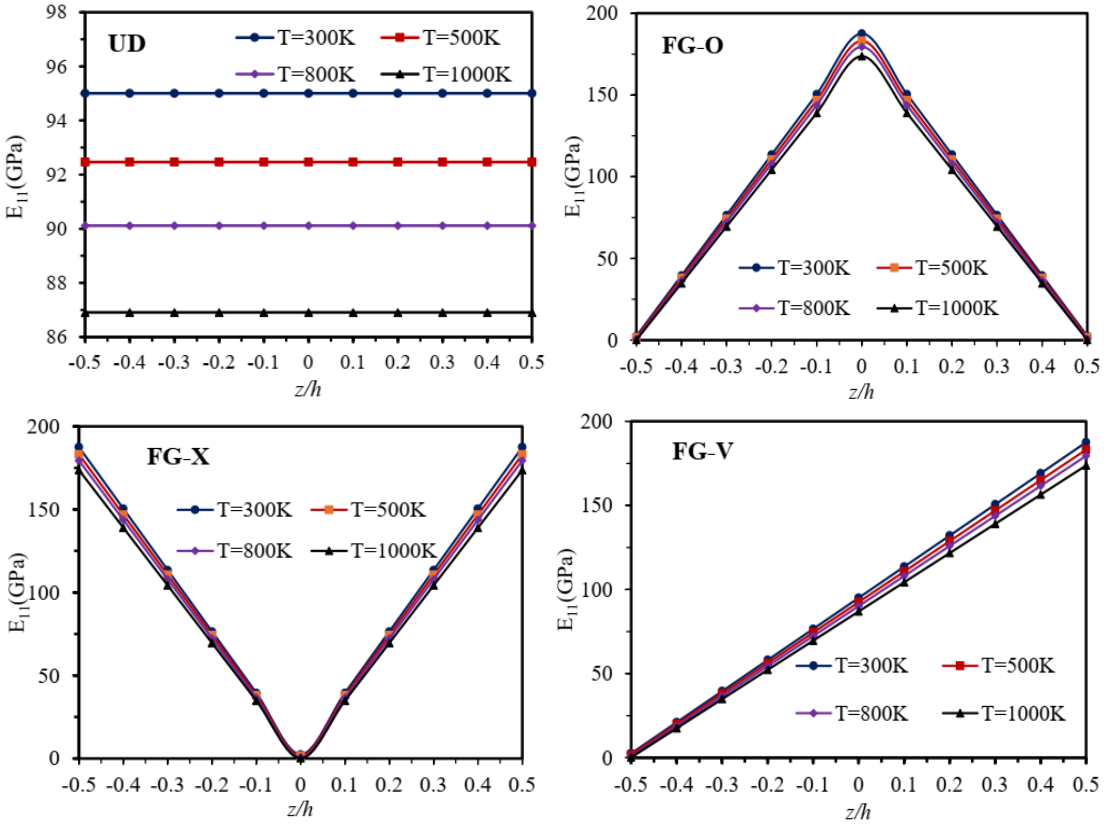

Fig. 2 The effective Young's modulus E_{11} of FG-CNTRC nanobeams, with $V_{CNT}^{*} = 0.12$ and $\Delta H = 0\%$

where E_0^m and ρ_0^m are values of E^m and ρ^m at room temperature ($T = 300K$) and moisture $H = 0$ [$\%wt.H_2O$], respectively.

4.1 Comparison studies

To validate the accuracy of the proposed model, the first three dimensionless natural frequencies of FG-O beams in thermal environment are compared with results obtained by Babaei *et al.* (2021) using a two-step perturbation technique. The results of the comparison are clearly summarized in Table 3. It is noted that the results of FG-CNTRC beams based on the classical elasticity theory can be retrieved from the present nonlocal elasticity framework by simply setting the nonlocal parameter equal to zero $e_0 a = 0$. In this study, the influence of the moisture concentration is ignored, and the length-to-thickness ratio is set equal to $L/h = 30$. The volume fraction of CNTs is set to $V_{CNT}^{*} = 0.17$. The obtained results show good agreement with the reference data. This confirms the validity and reliability of the present approach in predicting the vibrational behavior of FG-CNTRC beams.

4.2 Parametric studies

In this section, the influences of some key parameters on the free vibrational behavior of FG-

Table 3 A comparison of the first three dimensionless natural frequencies Ω_i of the FG-O beams with $L/h = 30$ and $V_{CNT}^* = 0.17$

Frequency	Source	$T = 300K$	$T = 320K$	$T = 340K$	$T = 360K$	$T = 380K$	$T = 400K$
Ω_1	Babaei *et al.* (2021)	14.3890	13.0675	11.4886	09.5493	6.9562	2.0515
	Present	14.4338	13.1187	11.5406	9.5970	7.0151	2.2006
Ω_2	Babaei *et al.* (2021)	52.9129	51.3224	49.5832	47.6926	45.6448	43.4305
	Present	53.0715	51.4855	49.7458	47.8511	45.7968	43.5745
Ω_3	Babaei *et al.* (2021)	106.220	104.034	101.689	99.1878	96.5310	93.7170
	Present	106.489	104.307	101.959	99.4495	96.7797	93.9500

Table 4 The effects of the nonlocal parameter, shear deformations, CNT distribution patterns, and moisture concentration on the first dimensionless natural frequency of the FG-CNTRC nanobeams with $L/h = 15$, $V_{CNT}^* = 0.12$ at $T = 300K$

e_0a/h	Theory	ΔH=0.1%				ΔH=0.2%			
		UD	FG-O	FG-X	FG-V	UD	FG-O	FG-X	FG-V
0.0	TBT	13.1164	9.7927	15.0023	13.1235	12.2296	8.5822	14.2251	12.2372
	SBT	13.1242	9.7777	15.0226	13.1307	12.2379	8.5651	14.2465	12.2449
	EBT	13.1405	9.7666	15.0559	13.1464	12.2555	8.5523	14.2817	12.2618
0.4	TBT	13.0647	9.7506	14.9448	13.0718	12.1743	8.5342	14.1646	12.1819
	SBT	13.0725	9.7357	14.9650	13.0790	12.1826	8.5171	14.1860	12.1896
	EBT	13.0887	9.7246	14.9982	13.0946	12.2001	8.5044	14.2210	12.2064
0.8	TBT	12.9128	9.6268	14.7757	12.9198	12.0114	8.3927	13.9865	12.0189
	SBT	12.9204	9.6120	14.7957	12.9269	12.0196	8.3757	14.0077	12.0266
	EBT	12.9365	9.6009	14.8286	12.9424	12.0370	8.3630	14.0425	12.0433
1.0	TBT	11.7268	9.1223	13.0818	11.7348	11.0900	8.3010	12.5066	11.0984
	SBT	11.7381	9.1048	13.1073	11.7454	11.1020	8.2818	12.5333	11.1097
	EBT	11.7594	9.0922	13.1472	11.7660	11.1246	8.2679	12.5750	11.1316

CNTRC nanobeams subjected to hygro-thermal environments are thoroughly investigated. Specifically, the effects of volume fraction of CNTs (V_{CNT}^*), CNT distribution patterns through the thickness (UD, FG-O, FG-X and FG-V), length-to-thickness ratio (*L/h*), dimensionless nonlocal parameter (e_0a/h), and variations in temperature and moisture concentration are examined in detail. This analysis aims to elucidate the complex interactions between material properties, geometric factors, and environmental conditions, thereby providing essential insights for the design and optimization of nano-composite structures operating in harsh service conditions. The obtained results offer a deeper understanding of the dynamic response of FG-CNTRC nanobeams and serve as a scientific foundation for practical applications in nano-engineering and advanced material systems.

The selection of the nonlocal parameter (e_0a) plays a pivotal role in accurately modeling the mechanical behavior of FG-CNTRC nanobeams using nonlocal elasticity theory. Zhang *et al.* (2005)

proposed determining the nonlocal parameter (e_0a) by aligning the theoretical buckling strain - predicted by a nonlocal thin shell model (Zhang 2004) - with the results from molecular mechanics simulations conducted by Sears and Batra (2004). This calibration yielded an estimated value of the nonlocal parameter e_0a of about 0.1 nm. Based on the frequency equation, Wang (2005) estimated the nonlocal parameter e_0a to be less than 2.10 nm for a CNT by substituting the available experimental vibration frequency of 0.1 THz (Wang 2005) Alternatively, assuming that the measured frequency exceeded 10 THz as reported by Yoon *et al.* (2004), the corresponding estimate for e_0a was refined to below 2.1nm. By comparing vibration frequencies and bending behavior of SWCNTs with lattice dynamics simulations, Reddy and Pang (2008) estimated value of the nonlocal parameter $e_0a \approx 0.39$nm. No universal value exists for values of the nonlocal parameter e_0a, as it strongly depends on the material type, structure size, boundary conditions, and the mechanical problem considered. To the authors' knowledge, up to now, there is no specific value of the nonlocal parameter for FG-CNTRC nanobeams. In the present analysis, the nonlocal parameter e_0a is normalized with respect to the nanobeam's thickness: e_0a/h. Its value is considered to vary from 0 to 1 to capture the influence of scale-dependent effects.

Table 4 lists the first dimensionless natural frequency (Ω) of the FG-CNTRC nanobeams for some values of the dimensionless nonlocal parameter ($e_0a/h = 0,0.4,0.8$ and 1.0). It is also considered three types of the shear deformation beam theory including TBT, SBT and EBT. It is assumed that the nanobeam is operating at room temperature ($T = 300K$). The variation in moisture concentration is considered in this calculation ($\Delta H = 0.1\%$ and $\Delta H = 0.2\%$). The length-to-thickness of the nanobeams is considered as $L/h = 15$. Results are shown for all four CNT distribution types (UD, FG-O, FG-X and FG-V), and the volume fraction of CNTs is considered $V_{CNT}^{*} = 0.12$. It can be observed that the negligible difference in the natural frequencies of the FG-CNTRC nanobeams when considering different shear deformation beam models. It can be observed that the increase in moisture concentration reduces the natural frequency of FG-CNTRC nanobeams. The stiffness-softening effect arising in the nanobeam can be observed, namely the increase in the nonlocal parameter leads to a decrease in the natural frequency of the FG-CNTRC nanobeams. The influence of different CNT distribution patterns (UD, FG-O, FG-V, and FG-X) on the natural dimensionless frequencies of FG-CNTRC nanobeams is evident through the numerical results given in Table 4. It is observed that the FG-X configuration yields the highest natural frequencies, whereas the FG-O configuration leads to the lowest ones. This behavior can be attributed to the distribution of CNTs in each pattern: in the FG-X model, a greater concentration of CNTs is located near the top and bottom surfaces, which are the regions experiencing maximum bending stresses. As a result, the flexural rigidity of the nanobeam is significantly enhanced. In contrast, the FG-O model concentrates CNTs near the mid-surface, contributing less effectively to the nanobeam's overall bending stiffness and thereby resulting in reduced natural frequencies.

In Table 5, the effects of temperature elevation and volume fraction of CNTs on the first three dimensionless natural frequencies of FG-CNTRC nanobeams are studied. In this study, the following parameters are used $L/h = 10$, $e_0a/h = 0.1$, and the influence of the variation in moisture concentration is ignored. The results indicate that the dimensionless natural frequencies of the FG-CNTRC nanobeams decrease with increasing temperature. This trend can be explained by the temperature-induced reduction in the elastic modulus of the constituent materials, which leads to a decline in the overall stiffness of the structure. In addition, the thermal environment generates compressive axial loads due to thermal expansion, which further diminishes the vibrational frequencies. These combined effects highlight the significant influence of thermal conditions on the dynamic behavior of FG-CNTRC nanobeams. It is also observed that the natural frequencies of the

Table 5 The effect of temperature variation, volume fraction of CNTs and CNT distribution patterns on the first three dimensionless natural frequencies of the FG-CNTRC nanobeams with $e_0a/h = 0.1,\ L/h = 10,$ and ΔH=0%

Distribution	V^*_{CNT}	T = 300K			T = 350K			T = 400K		
		Ω_1	Ω_2	Ω_3	Ω_1	Ω_2	Ω_3	Ω_1	Ω_2	Ω_3
UD	0.12	11.633	29.057	47.199	11.067	27.728	45.134	10.416	26.247	42.864
	0.17	14.513	36.912	60.098	13.857	35.317	57.576	13.105	33.546	54.814
	0.28	16.523	40.284	65.354	15.645	38.307	62.355	14.625	36.083	59.028
FG-O	0.12	9.5430	25.666	42.134	8.981	24.398	40.092	8.319	22.964	37.814
	0.17	11.826	32.727	54.250	11.185	31.243	51.799	10.432	29.570	49.078
	0.28	14.099	37.499	61.322	13.256	35.605	58.292	12.254	33.448	54.892
FG-X	0.12	12.650	30.246	48.829	12.056	28.875	46.748	11.379	27.357	44.471
	0.17	15.799	38.226	61.690	15.103	36.568	59.141	14.312	34.740	56.361
	0.28	17.423	40.718	65.992	16.501	38.710	63.027	15.439	36.460	59.748
FG-V	0.12	11.642	29.088	47.249	11.075	27.757	45.182	10.424	26.275	42.910
	0.17	14.535	36.997	60.245	13.880	35.401	57.720	13.129	33.630	54.954
	0.28	16.632	40.640	65.939	15.758	38.666	62.931	14.743	36.443	59.596

Table 6 The effects of nonlocal parameter and length-to-thickness ratio on the first dimensionless natural frequencies of the FG-CNTRC nanobeams, with $e_0a/h = 0.1,$ UD, $\Delta T = 0K, \Delta H = 0\%$

V^*_{CNT}	Model	*L/h*=5	*L/h*=10	*L/h*=20	*L/h*=30	*L/h*=40	*L/h*=50	*L/h=100*
0.12	TBT	7.2629	11.6318	15.1669	16.2748	16.7257	16.9478	17.25857
	SBT	7.3054	11.6471	15.1710	16.2766	16.7267	16.9485	17.2587
	EBT	7.3618	11.6735	15.1807	16.2815	16.7296	16.9503	17.2592
0.17	TBT	9.2274	14.5125	18.5087	19.7025	20.1799	20.4133	20.7377
	SBT	9.2738	14.5286	18.5129	19.7043	20.1809	20.4139	20.7379
	EBT	9.3367	14.5575	18.5233	19.7094	20.1839	20.4159	20.7384
0.28	TBT	10.0694	16.5209	22.2914	24.2435	25.0620	25.4706	26.0487
	SBT	10.1428	16.5488	22.2992	24.2469	25.0639	25.4718	26.0490
	EBT	10.2378	16.5946	22.3168	24.2559	25.0692	25.4753	26.0499

FG-CNTRC nanobeams increase with the enhancement of CNT volume fraction (V^*_{CNT}). This behavior is primarily due to the superior mechanical properties of CNTs compared to the matrix material. As the volume fraction of CNTs increases, the effective elastic modulus of the composite is significantly improved, leading to higher structural stiffness and, consequently, higher natural frequencies. The findings also demonstrate that the natural frequencies of the UD and FG-V nanobeams are nearly identical. This similarity can be attributed to the relatively uniform distribution of CNTs across the nanobeam thickness in both configurations. Although the FG-V pattern introduces a gradual variation in CNT concentration, the overall stiffness distribution remains close to that of the UD case, especially when the volume fraction of CNTs is moderate. As

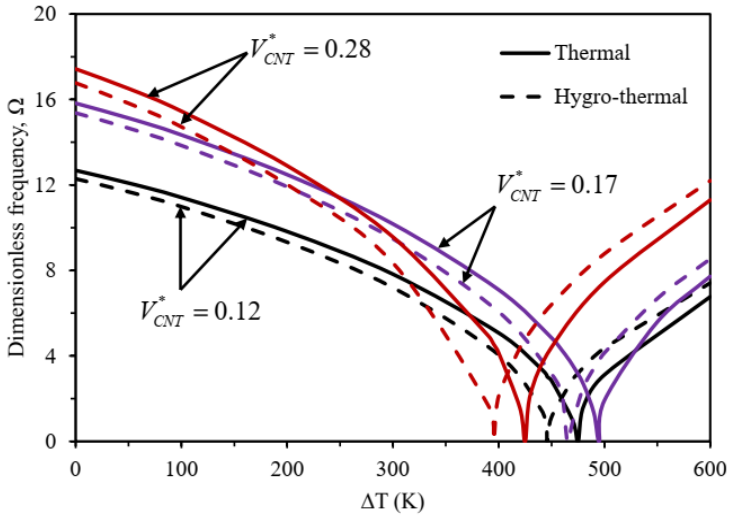

Fig. 3 The effect of volume fraction of CNTs on the first dimensionless natural frequency of FG-CNTRC nanobeams in hygro-thermal environments, (FG-X, *L/h*=10, $e_0 a/h = 0.1$)

a result, the effective mechanical properties and dynamic response of the nanobeam do not differ significantly between these two distributions.

The effect of the length-to-thickness ratio (*L/h*) on the first dimensionless natural frequencies of the FG-CNTRC nanobeams are shown in Table 6. The numerical results in Table 6 are given with $e_0 a/h = 0.1$ and UD distribution pattern of CNTs. The effects of the variation in temperature and moisture concentration were not considered in this study. The results further reveal that the dimensionless natural frequency of the nanobeam increases with an increase in the length-to-thickness ratio (*L/h*). This trend can be attributed to the geometric characteristics of slender beams, where an increase in *L/h* leads to a higher flexibility and a lower mass per unit length relative to stiffness, thereby resulting in elevated natural frequencies. This observation is consistent with the results of Babaei *et al.* (2021). The divergence is more pronounced in beams with smaller length-to-thickness ratios (*L/h*), indicating that the influence of certain parameters, such as nonlocal effects or shear deformation, is more significant in geometrically thicker nanobeams. From this table, it is evident that divergence becomes more pronounced when the length-to-thickness ratio (*L/h*) is small. When the nanobeam is slender (the large length-to-thickness ratio), the influence of shear deformation diminishes, and the predictions of different theories tend to converge.

The effect of the volume fraction of CNTs (V^*_{CNT}) on the free variation of FG-CNTRC nanobeams in hygro-thermal environments is investigated and presented in Fig. 3. Two elevated temperature conditions are considered, including thermal (ΔH=0%) and hygro-thermal (ΔH=0.1%) environments. The fundamental frequency of the nanobeam is presented for three different values of volume fraction of CNTs ($V^*_{CNT} = 0.12,\ 0.17$ and 0.28). It is observed that the natural frequencies decrease with increasing temperature up to a certain point, after which they begin to rise. In the initial phase, the nanobeam remains flat and is considered to be in the thermal pre-buckling state. During this stage, the increasing thermal load reduces the effective stiffness of the structure, leading to a gradual decrease in natural frequencies. This trend continues until the nanobeam reaches its critical buckling temperature, at which point the total stiffness approaches zero and the fundamental frequency tends

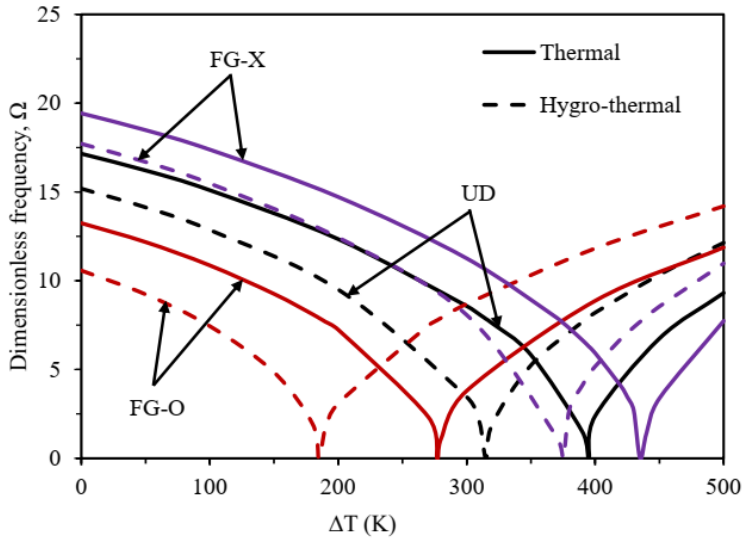

Fig. 4 The effect of CNT distribution pattern on the first dimensionless natural frequency of FG-CNTRC nanobeams in hygro-thermal environments, ($V^*_{CNT} = 0.17$, L/h=15, $e_0 a/h = 0.2$)

toward zero. Beyond this point, in the thermal post-buckling regime, further increases in temperature lead to a rise in natural frequencies due to the development of membrane forces and geometric stiffening associated with the post-buckled configuration. As observed, in the absence of thermal effects, an increase in the volume fraction of CNTs leads to a corresponding increase in the natural frequency, owing to the enhanced stiffness of the composite material. However, it is also noted that the nanobeam with an intermediate volume fraction of CNTs does not necessarily exhibit an intermediate critical buckling temperature. This indicates that the relationship between CNT content and thermal stability is nonlinear and may be influenced by the specific distribution pattern and coupling between mechanical and thermal responses. As observed in this example, the critical buckling temperature of the nanobeam with $V^*_{CNT} = 0.12$ is higher than that of the nanobeam with $V^*_{CNT} = 0.28$. This non-monotonic behavior suggests that increasing the CNT content does not always result in improved thermal stability, likely due to the complex interaction between CNT distribution, matrix properties, and the induced thermal stresses. The results also reveal that an increase in moisture concentration leads to a reduction in both the natural frequency and critical buckling temperature of the nanobeam. This behavior can be attributed to the hygroscopic degradation of the matrix material, which results in a reduction of the overall stiffness of the composite structure. Additionally, moisture absorption can induce internal swelling and micro/nano structural changes at the CNT–matrix interface, weakening the load transfer efficiency. These effects collectively diminish the nanobeam's resistance to both vibrational and thermal instability, highlighting the detrimental influence of humid environments on the mechanical performance of FG-CNTRC nanobeams.

Fig. 4 presents the effect of CNT distribution pattern on the free vibration of FG-CNTRC nanobeams in thermal environment ($\Delta H = 0\%$) and hygro-thermal environment ($\Delta H = 0.2\%$). The results indicate that the FG-X distribution yields the highest natural frequency, while the FG-O distribution results in the lowest. A similar trend is observed for the critical buckling temperature, where the FG-X configuration exhibits the highest value, followed by the UD type, and the FG-O

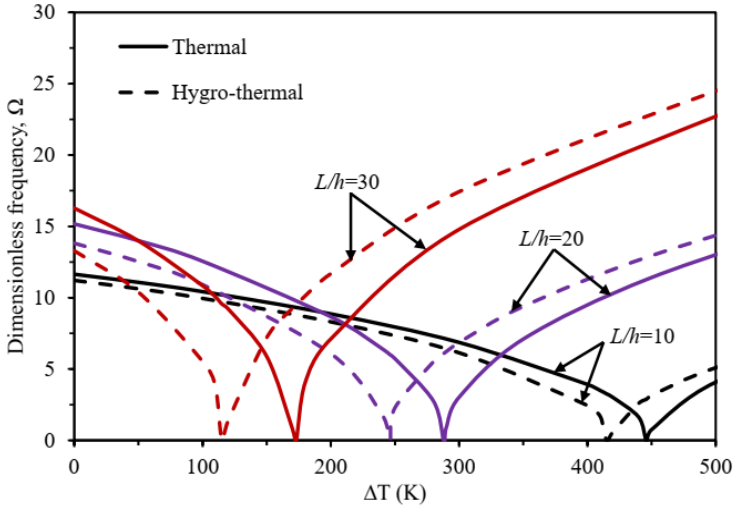

Fig. 5 The effect of length-to-thickness ratio on the first dimensionless natural frequency of FG-CNTRC nanobeams in hygro-thermal environments, ($V^*_{CNT} = 0.12$, FG-V, $e_0 a/h = 0.1$)

configuration shows the lowest. This behavior can be attributed to the variation in flexural rigidity associated with each distribution pattern. Specifically, the FG-X pattern, which concentrates CNTs near the outer surfaces, provides maximum resistance to bending, thereby enhancing both dynamic and thermal stability. In contrast, the FG-O pattern, with CNTs concentrated near the mid-surface, results in the lowest flexural rigidity. The UD configuration offers intermediate performance in both natural frequency and buckling resistance.

The impact of length-to-thickness ratio (L/h) on the free vibration of FG-CNTRC nanobeams in thermal environment ($\Delta H = 0\%$) and hygro-thermal environment ($\Delta H = 0.1\%$) can be observed in Fig. 5. It is observed that the critical buckling temperature of the nanobeam increases as the length-to-thickness ratio (L/h) decreases. This trend can be explained by the fact that the nanobeams with smaller length-to-thickness ratios are geometrically stiffer, exhibiting higher flexural rigidity. As a result, they are more resistant to thermally induced compressive loads, leading to higher critical buckling temperatures. This observation underscores the significant role of geometric parameters in the thermal stability of FG-CNTRC nanobeams and suggests that thickness optimization can be an effective design strategy for enhancing buckling resistance under elevated temperature environments.

The influence of the nonlocal parameter ($e_0 a/h$) on the free vibration of FG-CNTRC nanobeams is presented in Fig. 6. In this study, the nanobeam are assumed to operate at a temperature of T=350K, the effect of variation in moisture concentration is considered ΔH=0.2%. The results demonstrate that the dimensionless natural frequencies of the nanobeam decrease as the nonlocal parameter increases. This behavior reflects the inherent size-dependent nature of nonlocal elasticity theory, in which the stress at a given point is influenced by strains over a surrounding region. As the nonlocal parameter increases, the material exhibits a softer mechanical response, effectively reducing the stiffness of the structure. Consequently, this leads to a reduction in the natural frequencies, emphasizing the importance of accounting for small-scale effects in the dynamic analysis of FG-CNTRC nanobeams.

The findings of this study provide valuable insights for the design and optimization of MEMS/

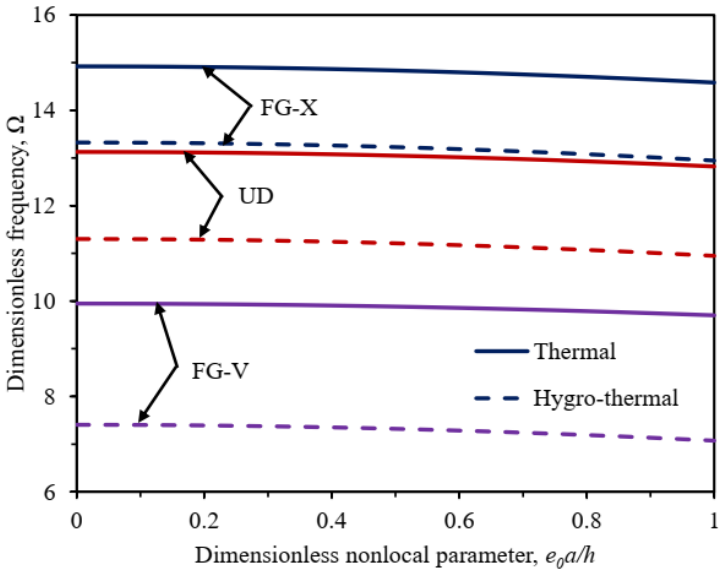

Fig. 6 The effect of nonlocal parameter on the first dimensionless natural frequency of FG-CNTRC nanobeams in hygro-thermal environments, ($V^*_{CNT} = 0.12$, L/h=15)

NEMS devices, particularly those employing FG-CNTRC nanostructures as sensing or actuation elements. The demonstrated sensitivity of the natural frequencies to hygro-thermal conditions suggests that such nanobeams can be utilized as environmental sensors capable of detecting subtle changes in temperature or moisture. Moreover, the ability to tune vibrational characteristics through CNT distribution patterns and volume fractions enables tailored performance in frequency-selective devices such as resonators or filters. The incorporation of the NET ensures the model's suitability for capturing size-dependent effects, which are crucial in nanoscale applications.

4. Conclusions

In this study, an analytical investigation into the free vibration characteristics of FG-CNTRC nanobeams under hygro-thermal conditions was conducted, based on a refined shear deformation beam theory combined with nonlocal elasticity theory, providing deeper insights into their dynamic responses. The extended rule of mixtures is utilized to predict the effective material properties, incorporating temperature dependence and various CNT distribution patterns, including uniform and three functionally graded configurations. Based on the comprehensive analysis, the following key conclusions are drawn:

• The refined shear deformation theory significantly enhances the accuracy in capturing size-dependent behaviors and shear effects, particularly for thick nanobeams.

• Among the CNT distribution profiles, the FG-X pattern yields the highest natural frequencies and critical buckling temperatures due to its greater flexural rigidity, while the FG-O pattern results in the lowest.

• The natural frequencies increase with a higher CNT volume fraction but decrease with rising temperature, moisture content, and nonlocal parameter values.

• In the pre-buckling regime, the natural frequencies decline as the temperature increases, whereas in the post-buckling regime, they rise with further temperature elevation.

• The nanobeams with intermediate CNT volume fractions do not necessarily demonstrate intermediate critical buckling temperatures.

Overall, this study emphasizes the crucial role of shear deformation, nonlocal effects, material gradation, and hygro-thermal conditions in accurately predicting the dynamic response of FG-CNTRC nanobeams. The findings provide valuable insights for the optimal design and performance evaluation of advanced nanostructures in engineering applications.

In future studies, the proposed framework can be extended to incorporate coupled multi-physical effects such as electromagnetic, piezoelectric, and magneto-thermal interactions. These phenomena are highly relevant in the design of smart nanostructures and multifunctional MEMS/NEMS devices, where external fields significantly influence the mechanical behavior at small scales.

Acknowledgments

The authors gratefully acknowledge the support provided by Phenikaa University.

Author contributions

Conceptualization: Dang Van Hieu, Nguyen Thi Hoa, Bui Gia Phi; Methodology: Dang Van Hieu, Nguyen Thi Hoa, Nguyen Thi Kim Thoa; Formal Analysis: Dang Van Hieu, Nguyen Thi Hoa, Nguyen Thi Kim Thoa, Bui Gia Phi; Investigation: Dang Van Hieu, Nguyen Thi Hoa; Writing – Original Draft Preparation: Dang Van Hieu, Nguyen Thi Kim Thoa; Writing – Review & Editing: Dang Van Hieu, Nguyen Thi Hoa, Nguyen Thi Kim Thoa, Bui Gia Phi.

References

Abdelrahman, A.A., Esen, I., Daikh, A.A. and Eltaher, M.A. (2023), "Dynamic analysis of FG nanobeam reinforced by carbon nanotubes and resting on elastic foundation under moving load", *Mech. Based Des. Struct. Mach.*, **51**(10), 5383-5406. https://doi.org/10.1080/15397734.2021.1999263

Algamili, A.S., Khir, M.H.M., Dennis, J.O., Ahmed, A.Y., Alabsi, S.S., Ba Hashwan, S.S. and Junaid, M.M. (2021), "A review of actuation and sensing mechanisms in MEMS-based sensor devices", *Nanosc. Res. Lett.*, **16**, 16. https://doi.org/10.1186/s11671-021-03481-7

Allahkarami, F. and Nikkhah-Bahrami, M. (2017), "The effects of agglomerated CNTs as reinforcement on the size-dependent vibration of embedded curved microbeams based on modified couple stress theory", *Mech. Adv. Mater. Struct.*, **25**(12), 995-1008. https://doi.org/10.1080/15376494.2017.1323144

Anh, V.T.T., Dat, N.D., Nguyen, P.D. and Duc, N.D. (2024), "A nonlocal higher-order shear deformation approach for nonlinear static analysis of magneto-electro-elastic sandwich Micro/Nano-plates with FG-CNT core in hygrothermal environment", *Aerosp. Sci. Technol.*, **147**, 109069. https://doi.org/10.1016/j.ast.2024.109069

Anumandla, V. and Gibson, R.F. (2006), "A comprehensive closed form micromechanics model for estimating the elastic modulus of nanotube-reinforced composites", *Compos. Part A*, **37**(12), 2178-2185. https://doi.org/10.1016/j.compositesa.2005.09.016

Arani, A.G., Pourjamshidian, M., Arefi, M. and Arani, M.R.G. (2019), "Thermal electrical and mechanical buckling loads of sandwich nano-beams made of FG-CNTRC resting on Pasternak's foundation based on

higher order shear deformation theory", *Struct. Eng. Mech.*, **69**(4), 439-455. https://doi.org/10.12989/sem.2019.69.4.439

Arefi, M., Pourjamshidian, M. and Arani, A.G. (2019), "Dynamic instability region analysis of sandwich piezoelectric nano-beam with FG-CNTRCs face-sheets based on various high-order shear deformation and nonlocal strain gradient theory", *Steel Compos. Struct.*, **32**(2), 151-171. https://doi.org/10.12989/scs.2019.32.2.151

Babaei, H., Kiani, Y. and Eslami, M.R. (2021), "Vibrational behavior of thermally pre-/post-buckled FG-CNTRC beams on a nonlinear elastic foundation: a two-step perturbation technique", *Acta Mechanica*, **232**, pp. 3897–3915. https://doi.org/10.1007/s00707-021-03027-z

Belarbi, M.O., Salami, S.J., Garg, A., Daikh, A.A., Houari, M.S.A., Dimitri, R. and Tornabene, F. (2023), "Mechanical behavior analysis of FG-CNT-reinforced polymer composite beams via a hyperbolic shear deformation theory", *Continuum Mech. Thermodyn.*, **35**, 497-520. https://doi.org/10.1007/s00161-023-01191-2

Bhat, A., Budholiya, S., Raj, S.A., Sultan, M.T.H., Hui, D., Shah, A.U.M. and Safri, S.N.A. (2021), "Review on nanocomposites based on aerospace applications", *Nanotechnol. Rev.*, **10**(1), 237-253. https://doi.org/10.1515/ntrev-2021-0018

Borjalilou, V., Taati, E. and Ahmadian, M.T. (2019), "Bending, buckling and free vibration of nonlocal FG-carbon nanotube-reinforced composite nanobeams: exact solutions", *SN Appl. Sci.*, **1**, 1323. https://doi.org/10.1007/s42452-019-1359-6

Chandel, V.S., Wang, G. and Talha, M. (2020), "Advances in modelling and analysis of nano structures: A review", *Nanotechnol. Rev.*, **9**(1), 230-258. https://doi.org/10.1515/ntrev-2020-0020

Coleman, J.N., Khan, U., Blau, W.J., Gun'ko, Y.K. (2006), "Small but strong: a review of the mechanical properties of carbon nanotube-polymer composites", *Carbon*, **44**, 1624-1652. https://doi.org/10.1016/j.carbon.2006.02.038

Dehkordi, H.R.B. and Beni, Y.T. (2023), "Size-dependent coupled bending-torsional vibration of functionally graded carbon nanotube reinforced composite Timoshenko microbeams", *Arch. Civil Mech. Eng.*, **23**, 186. https://doi.org/10.1007/s43452-023-00725-4

Ebrahimi, F. and Barati, M.R. (2026), "A unified formulation for dynamic analysis of nonlocal heterogeneous nanobeams in hygro-thermal environment", *Appl. Phys. A*, **122**, 792. https://doi.org/10.1007/s00339-016-0322-2

Eringen, A.C. (1983), "On differential equations of nonlocal elasticity and solutions of screw dislocation and surface waves", *J. Appl. Phys. AIP Publishing*, **54**, 4703-4710. https://doi.org/10.1063/1.332803

Esawi, A.M.K. and Farag, M.M. (2007), "Carbon nanotube reinforced composites: Potential and current challenges", *Mater. Des.*, **28**, 2394-2401. https://doi.org/10.1016/j.matdes.2006.09.022

Farajpour, A., Ghayesh, M.H. and Farokhi, H. (2018), "A review on the mechanics of nanostructures", *Int. J. Eng. Sci.*, **133**, 231-263. https://doi.org/10.1016/j.ijengsci.2018.09.006

Forooghi, A. and Alibeigloo, A. (2022), "Hygro-thermo-magnetically induced vibration of FG-CNTRC small-scale plate incorporating nonlocality and strain gradient size dependency", *Waves Random Complex Med.*, **35**(1), 1718-1749. https://doi.org/10.1080/17455030.2022.2037784

Gia Phi, B., Van Hieu, D., Sedighi, H.M. and Sofiyev, A.H. (2022), "Size-dependent nonlinear vibration of functionally graded composite micro-beams reinforced by carbon nanotubes with piezoelectric layers in thermal environments", *Acta Mechanica*, **233**, 2249-2270. https://doi.org/10.1007/s00707-022-03224-4

Hughes, K.J., Iyer, K.A., Bird, R.E., Ivanov, J., Banerjee, S., Georges, G. and Zhou, Q.A. (2024), "Review of carbon nanotube research and development: Materials and emerging applications", *ACS Appl. Nano Mater.*, **7**(16), 18695-18713. https://doi.org/10.1021/acsanm.4c02721

Iijima, S. (1991), "Helical microtubules of graphitic carbon", *Nature*, **354**(6348), 56. https://doi.org/10.1038/354056a0

Jamali, M., Shojaee, T., Mohammadi, B. and Kolahchi, R. (2019), "Cut out effect on nonlinear post-buckling behavior of FG-CNTRC micro plate subjected to magnetic field via FSDT", *Adv. Nano Res.*, **7**(6), 405-417. https://doi.org/10.12989/anr.2019.7.6.405

Ke, L.L., Yang, J. and Kitipornchai, S. (2010), "Nonlinear free vibration of functionally graded carbon

nanotube-reinforced composite beams", *Compos. Struct.*, **92**, 676-683. https://doi.org/10.1016/j.compstruct.2009.09.024

Khan, F., Hossain, N., Mim, J.J., Rahman, S.M.M., Iqbal, M.J., Billah, M. and Chowdhury, M.A. (2024), "Advances of composite materials in automobile applications - A review", *J. Eng. Res.*, **13**(2), 1001-1023. https://doi.org/10.1016/j.jer.2024.02.017

Kolahdouzan, F., Arani, A.G. and Abdollahian, M. (2018), "Buckling and free vibration analysis of FG-CNTRC-micro sandwich plate", *Steel Compos. Struct.*, **26**(3), 273-287. https://doi.org/10.12989/scs.2018.26.3.273

Kolahdouzan, F., Mosayyebi, M., Ghasemi, F.A., Kolahchi, R. and Panah, S.R.M. (2020), "Free vibration and buckling analysis of elastically restrained FG-CNTRC sandwich annular nanoplates", *Adv. Nano Res.*, **9**(4), 237-250. https://doi.org/10.12989/anr.2020.9.4.237

Li, L., Shi, Z., Peng, W. and He. T. (2024), "Thermoelastic bending wave propagation of FG hybrid nanocomposite microbeam reinforced by GPLs and CNTs under fractional order nonlocal elasticity theory", *J. Therm. Stress.*, **47**(11), 1500-1518. https://doi.org/10.1080/01495739.2024.2415027

Li, X., Gao, H., Scrivens, W.A., Fei, D., Xu, X., Sutton, M.A., Reynolds, A.P. and Myrick, M.L. (2007), "Reinforcing mechanisms of single-walled carbon nanotube-reinforced polymer composites", *J. Nanosci. Nanotechnol.*, **7**(7), 2309-2317. https://doi.org/10.1166/jnn.2007.410

Li, Y.S., Liu, B.L. and Zhang, J.J. (2021), "Hygro-thermal buckling of porous FG nanobeams considering surface effects", *Struct. Eng. Mech.*, **79**(3), 359-371. https://doi.org/10.12989/sem.2021.79.3.359

Lim, C.W., Zhang, G. and Reddy, J.N. (2015), "A higher-order nonlocal elasticity and strain gradient theory and its applications in wave propagation", *J. Mech. Phys. Solids*, **78**, 298-313. https://doi.org/10.1016/j.jmps.2015.02.001

Limongi, T., Tirinato, L., Pagliari, F., Giugni, A., Allione, M., Perozziello, G., Candeloro, P. and Di Fabrizio, E. (2017), "Fabrication and applications of micro/nanostructured devices for tissue engineering", *Nano Micro Lett.*, **9**(1), 1. https://doi.org/10.1007/s40820-016-0103-7

Lin, B., Chen, B., Zhu, B., Li, J. and Li, Y. (2021), "Dynamic stability analysis for rotating pre-twisted FG-CNTRC beams with geometric imperfections restrained by an elastic root in thermal environment", *Thin Wall. Struct.*, **164**, 107902. https://doi.org/10.1016/j.tws.2021.107902

Lin, F. and Xiang, Y. (2014), "Numerical analysis on nonlinear free vibration of carbon nanotube reinforced composite beams", *Int. J. Struct. Stabil. Dyn.*, **14**, 1350056. https://doi.org/10.1142/S0219455413500569

Mindlin, R.D. (1964), "Micro-structure in linear elasticity", *Arch. Ration. Mech. Anal.*, **16**(1), 51-78. https://doi.org/10.1007/BF00248490

Mindlin, R.D. (1965), "Second gradient of strain and surface-tension in linear elasticity", *Int. J. Solids Struct.*, **1**(4), 417-438. https://doi.org/10.1016/0020-7683(65)90006-5

Mindlin, R.D. and Eshel, N.N. (1968), "On first strain-gradient theories in linear elasticity", *In. J. Solids Struct.*, **4**(1), 109-124. https://doi.org/10.1016/0020-7683(68)90036-X

Owais, T., Khater, M. and Al-Qahtani, H. (2024), "Graphene-based MEMS devices for gas sensing applications: A review", *Micro Nanostruct.*, **195**, 207954. https://doi.org/10.1016/j.micrna.2024.207954

Pachkawade, V. (2024), "Transduction in M/NEMS—Actuation and Sensing: A Review", *IEEE Sensors J.*, **24**(6), 7420-7431. https://doi.org/10.1109/JSEN.2024.3356562

Penna, R., Feo, L. and Lovisi, G. (2021), "Hygro-thermal bending behavior of porous FG nano-beams via local/nonlocal strain and stress gradient theories of elasticity", *Compos. Struct.*, **263**, 113627. https://doi.org/10.1016/j.compstruct.2021.113627

Pham, Q.H., Nguyen, P.C. and Tran, V.K. (2024), "Effects of hygro-thermal environment on dynamic responses of variable thickness functionally graded porous microplates", *Steel Compos. Struct.*, **50**(5), 563-581. https://doi.org/10.12989/scs.2024.50.5.563

Pham, Q.H., Tran, V.K. and Nguyen, P.C. (2023), "Nonlocal strain gradient finite element procedure for hygro-thermal vibration analysis of bidirectional functionally graded porous nanobeams", *Waves Random Complex Med.*, 1-32. https://doi.org/10.1080/17455030.2023.2186708

Rao, R.K., Gautham, S. and Sasmal, S. (2024), "A comprehensive review on carbon nanotubes based smart nanocomposites sensors for various novel sensing applications", *Polym. Rev.*, **64**(2), 575-638.

https://doi.org/10.1080/15583724.2024.2308889
Reddy, J.N. and Pang, S.D. (2008), "Nonlocal continuum theories of beams for the analysis of carbon nanotubes", *J. Appl. Phys.*, **103**(2), 023511. https://doi.org/10.1063/1.2833431
Roudbari, M.A., Jorshari, T.D., Lü, C., Ansari, R., Kouzani, A.Z. and Amabilim, M. (2022), "A review of size-dependent continuum mechanics models for micro- and nano-structures", *Thin Wall. Struct.*, **170**, 108562. https://doi.org/10.1016/j.tws.2021.108562
Sears, A. and Batra, R.C. (2004), "Macroscopic properties of carbon nanotubes from molecular-mechanics simulations", *Phys. Rev. B*, **69**, 235406. https://doi.org/10.1103/PhysRevB.69.235406
Seidel, G.D. and Lagoudas, D.C. (2006), "Micromechanical analysis of the effective elastic properties of carbon nanotube reinforced composites", *Mech. Mater.*, **38**, 884-907. https://doi.org/10.1016/j.mechmat.2005.06.029
Shen, H.S. (2009), "Nonlinear bending of functionally graded carbon nanotube-reinforced composite plates in thermal environments", *Compos. Struct.*, **91**(1), 9-19. https://doi.org/10.1016/j.compstruct.2009.04.026
Shen, H.S. (2016), "Postbuckling of nanotube-reinforced composite cylindrical panels resting on elastic foundations subjected to lateral pressure in thermal environments", *Eng. Struct.*, **122**, 174-183. https://doi.org/10.1016/j.engstruct.2016.05.004
Shen, H.S. and Xiang, Y. (2023), "Nonlinear analysis of nanotube-reinforced composite beams resting on elastic foundations in thermal environments", *Eng. Struct.*, **56**, 698-708. https://doi.org/10.1016/j.engstruct.2013.06.002
Taati, E., Borjalilou, V., Fallah, F. and Ahmadian, M.T. (2022), "On size-dependent nonlinear free vibration of carbon nanotube-reinforced beams based on the nonlocal elasticity theory: Perturbation technique", *Mech. Based Des. Struct. Mach.*, **50**(6), 2124-2146. https://doi.org/10.1080/15397734.2020.1772087
Thostenson, E.T., Ren, Z. and Chou, T.W. (2001), "Advances in the science and technology of carbon nanotubes and their composites: A review", *Compos. Sci. Technol.*, **61**, 1899-1912. https://doi.org/10.1016/S0266-3538(01)00094-X
Uzun, B. and Yaylı, M.Ö. (2024), "Free vibration of a carbon nanotube-reinforced nanowire/nanobeam with movable ends", *J. Vib. Eng. Technol.*, **12**, 6847-6863. https://doi.org/10.1007/s42417-024-01287-2
Vo-Duy, T., Ho-Huu, V. and Nguyen-Thoi, T. (2019), "Free vibration analysis of laminated FG-CNT reinforced composite beams using finite element method", *Front. Struct. Civil Eng.*, **13**, 324-336. https://doi.org/10.1007/s11709-018-0466-6
Wang, Q. (2005), "Wave propagation in carbon nanotubes via nonlocal continuum mechanics", *J. Appl. Phys.*, **98**, 124301. https://doi.org/10.1063/1.2141648
Wang, Y., Guo, J., Xu, D., Gu, Z. and Zhao, Y. (2023), "Micro-/nano-structured flexible electronics for biomedical applications", *Biomed. Technol.*, **2**, 1-14. https://doi.org/10.1016/j.bmt.2022.11.013
Xu, J., Yang, Z., Yang, J., Li, Y. (2021), "Free vibration analysis of rotating FG-CNT reinforced composite beams in thermal environments with general boundary conditions", *Aerosp. Sci. Technol.*, **118**, 107030. https://doi.org/10.1016/j.ast.2021.107030
Yang, F., Chong, A.C.M., Lam, D.C.C. and Tong, P. (2002), "Couple stress based strain gradient theory for elasticity", *Int. J. Solids Struct.*, **39**(10), 2731-2743. https://doi.org/10.1016/S0020-7683(02)00152-X
Yang, J., Huang, X.H. and Shen, H.S. (2020), "Nonlinear flexural behavior of temperature-dependent FG-CNTRC laminated beams with negative Poisson's ratio resting on the Pasternak foundation", *Eng. Struct.*, **207**, 110250. https://doi.org/10.1016/j.engstruct.2020.110250
Yang, W.D., Kang, W.B. and Wang, X. (2017), "Scale-dependent pull-in instability of functionally graded carbon nanotubes-reinforced piezoelectric tuning nano-actuator considering finite temperature and conductivity corrections of Casimir force", *Compos. Struct.*, **176**, 460-470. https://doi.org/10.1016/j.compstruct.2017.05.014
Yang, W.D., Yang, F.P. and Wang, X. (2016), "Coupling influences of nonlocal stress and strain gradients on dynamic pull-in of functionally graded nanotubes reinforced nano-actuator with damping effects", *Sensors Actuat. A Phys.*, **248**, 10-21. https://doi.org/10.1016/j.sna.2016.07.017
Yoon, J., Ru, C.Q. and Mioduchowski, A. (2004), "Timoshenko-beam effects on transverse wave propagation in carbon nanotubes", *Compos. Part B Eng.*, **35**(2), 87-93.

https://doi.org/10.1016/j.compositesb.2003.09.002
Zhang, N., Wang, Z., Zhao, Z., Zhang, D., Feng, J., Yu, L., Lin, Z., Guo, Q., Huang, J., Mao, J. and Yang, J. (2023), "3D printing of micro-nano devices and their applications", *Microsyst. Nanoeng.*, **11**, 35. https://doi.org/10.1038/s41378-024-00812-3
Zhang, P., Schiavone, P. and Qing, H. (2023), "Dynamic stability analysis of porous functionally graded beams under hygro-thermal loading using nonlocal strain gradient integral model", *Appl. Math. Mech.*, **44**, 2071-2092. https://doi.org/10.1007/s10483-023-3059-9
Zhang, Q., Uchaker, E., Candelaria, S.L. and Cao, G. (2013), "Nanomaterials for energy conversion and storage", *Chem. Soc. Rev.*, **42**, 3127-3171. https://doi.org/10.1039/C3CS00009E
Zhang, W.M., Yan, H., Peng, Z.K. and Meng, G. (2014), "Electrostatic pull-in instability in MEMS/NEMS: A review", *Sensors Actuat. A*, **214**, 187-218. https://doi.org/10.1016/j.sna.2014.04.025
Zhang, Y.Q., Liu, G.R. and Wang, J.S. (2004), "Small-scale effects on buckling of multiwalled carbon nanotubes under axial compression", *Phys. Rev. B*, **70**, 205430. https://doi.org/10.1103/PhysRevB.70.205430
Zhang, Y.Q., Liu, G.R. and Xie, X.Y. (2005), "Free transverse vibrations of double-walled carbon nanotubes using a theory of nonlocal elasticity", *Phys. Rev. B*, **71**, 195404. https://doi.org/10.1103/PhysRevB.71.195404
Zhao, J., Li, X., Li, S., Liu, Y. and Mohammadi. R. (2022), "Size-dependent investigation of the 2D-FG CNTRC nanobeams using nonlocal strain gradient beam theory subjected to hygro-thermo conditions", *Waves Random Complex Med.*, 1-20. https://doi.org/10.1080/17455030.2022.2070682

CC

Graphical abstract